

THERMAL PROPERTIES OF POLYLACTIDES

Effect of molecular mass and nature of lactide isomer

J. Ahmed, J.-X. Zhang, Z. Song and S. K. Varshney*

Polymer Source, Inc. 124 Avro street, Dorval, Montreal, Quebec, H9P 2X8, Canada

A thermal analysis of a series of polylactides (PLA) was carried out based on the number of average molecular mass (M_n), and the nature of isomer (*D*, *L* and *DL*). It is confirmed that the glass transition temperature (T_g) of PLA increased as a function of molecular mass irrespective of isomer type except sample with a high polydispersity index. The melting temperature (T_m) and enthalpy of crystal fusion (ΔH_f) of *L*-isomer increased as the M_n was increased from 1100 to 27500. The degree of crystallinity ($\chi_c\%$) increased as a function of molecular mass. However no crystallization peak was detected in the lower molecular mass range (550–1400). The non-isothermal crystallization behavior of the PLA melt was significantly influenced by the cooling rate. Both *D* and *L* isomers exhibited insignificant difference in thermal properties and *DL* lactides exhibited amorphous behavior at identical molecular masses. Change in microstructure showed significant difference between two isomers. Analysis of the FTIR spectra of these PLA samples in the range of 1200–1230 cm^{-1} supported DSC observation on crystallinity.

Keywords: crystallinity, glass transition temperature, melting temperature, polylactides

Introduction

Lactic acid based polymers are known as polylactides (PLA). The interests in polylactides have increased significantly due to their biodegradability and biocompatibility [1, 2]. Polylactide is used in various medical applications including as carriers for controlled release drug delivery systems, and in biodegradable pins, screws, and cell scaffolds in tissue engineering. Recently, polyanhydrides based on PLA have been accepted for implantations. These are included in architecturally fabricated fully bio-absorbable coronary stents for treating vascular disease, thus replacing conventional metallic stents [3]. These bio-absorbable stents are deployed as present stent. Furthermore, they utilize an anti-inflammatory, therapeutic drug-delivery polymer permitting delivery of multiple drugs with tunable release kinetics. The stent acts like a scaffold for tissue growth during the initial six months. Once the artery has healed, the stent is absorbed by the body, leaving no permanent implant. The advantage of polylactide based biopolymers over conventional metallic or non-biodegradable polymers is to ease of removal by the body system itself and retention of shape during time. Attention is also paid to PLA due to solid waste accumulation [4] and thus, there are significant efforts to produce newer biodegradable packaging materials based on PLA.

Because of the chirality of the lactyl unit, lactide exists in three diastereoisomeric forms: *L*-lactide,

D-lactide and meso-lactide. An equimolar mixture of *D* and *L* isomer results in *DL*-lactide. Among the various polylactides, optically pure polylactides, poly(*L*-lactide) (PLLA) and poly(*D*-lactide) (PDLA), are crystalline polymers with a melting point around 180°C [5, 6]. The atactic polymer, poly-(*DL*-lactide) is an amorphous material with a glass transition temperature of 50–57°C [7, 8]. It is well established that the properties of polylactides vary to a large extent depending on the ratio and the distribution of the two isomers.

In recent years there has been renewed interest in the crystallization of lactides. Nature derived lactides (agricultural source) are mostly in *L*-form and exhibit crystalline behavior. The crystallization of behavior of polylactides depends on the thermal history (i.e. annealing) [9], amount and type of additives [10] and stereo sequence distribution [11]. In addition, crystallization depends upon optical purity. It is reported that at least 72% threshold optical purity in composition is required to obtain crystallinity of polylactides [11, 12]. Semi-crystalline nature of PLA has been observed during cooling of melt [13]. The heat of crystallization measured by differential scanning calorimetry may depend on the stereosequence distribution in the polymer. It is also important to know the percent of crystallinity since it strongly influences the physical properties of the polymer and composite [14, 15].

Understanding of thermodynamic properties of lactides requires quantitative thermal analysis and reliable interpretation of the underlying molecular

* Author for correspondence: contact@polymersource.com

mobility [16]. Interestingly, polylactides exhibit both amorphous and semi-crystallinity and therefore a wide variation in thermal properties are expected for polylactides. Numerous publications are available on thermal properties and crystallinity of polylactides, but most of those studies have carried out with limited number of samples. An attempt is made to present a broad spectrum of thermal characteristics using a series of polylactides (*L*, *D* and *LD*) synthesized in our laboratory.

The main objectives of the present study is to investigate thermal properties (melting, crystallization and glass transition) of polylactides using calorimetric technique as function of molecular mass, isomer, and microstructure. In addition, the effect of cooling rate on melt crystallization behavior during non-isothermal cooling of *L*-lactides has also been investigated.

Experimental

Materials

Lactide monomer was obtained from Purac Co. USA and used as received. Both poly *L*(-), *D*(+) and racemic (*DL*±)-lactides were synthesized by tin-catalyzed ring-opening bulk polymerization. Diethylene glycol monomethyl ether, ethylene glycol and diethylene glycol were used as initiators. The obtained polymers were purified by dissolving in acetone and further precipitated in ethanol/hexane 2:8 v/v mixture. The precipitation repeated thrice to remove un-reacted lactide monomer. FTIR was used to ensure the complete removal of unreacted lactide monomer from the polymer by measuring a characteristic absorbance peak at 1250 cm⁻¹ assigned for the cyclic monomer structure. Finally samples were oven-dried at 38°C under vacuum for 48 h.

Table 1a Characteristics of PLA (*L*-form) samples: heating rate (10°C min⁻¹)

Product ID	M_n ·10 ³	M_w / M_n	T_g / °C	T_m / °C	ΔH / J g ⁻¹	T_c / °C	ΔH / J g ⁻¹	χ_c / %
P7163-(PLLA1)	0.55	1.30	-3.81	-	-	-	-	-
$\text{CH}_2\text{-O-CH}_2\text{-CH}_2\text{-O-CH}_2\text{-CH}_2\text{-O-}\left[\text{C}\begin{array}{c} \text{O} \\ \parallel \\ \text{C} \end{array}\text{-CH}\begin{array}{c} \text{CH}_3 \\ \end{array}\text{-O}\right]_n\text{-H}$ P7158-(PLLA2)	1.1	1.08	21.96	88.02	23.44	-	-	-
$\text{CH}_2\text{-O-CH}_2\text{-CH}_2\text{-O-CH}_2\text{-CH}_2\text{-O-}\left[\text{C}\begin{array}{c} \text{O} \\ \parallel \\ \text{C} \end{array}\text{-CH}\begin{array}{c} \text{CH}_3 \\ \end{array}\text{-O}\right]_n\text{-H}$ P7150-(PLLA3)	1.4	1.12	30.75	112.27	41.02	-	-	-
$\text{CH}_2\text{-O-CH}_2\text{-CH}_2\text{-O-CH}_2\text{-CH}_2\text{-O-}\left[\text{C}\begin{array}{c} \text{O} \\ \parallel \\ \text{C} \end{array}\text{-CH}\begin{array}{c} \text{CH}_3 \\ \end{array}\text{-O}\right]_n\text{-H}$ P3937-(PLLA4)	4.7	1.09	45.60	157.82	55.50	98.25	47.82	8.26
$\text{CH}_2\text{-O-CH}_2\text{-CH}_2\text{-O-CH}_2\text{-CH}_2\text{-O-}\left[\text{C}\begin{array}{c} \text{O} \\ \parallel \\ \text{C} \end{array}\text{-CH}\begin{array}{c} \text{CH}_3 \\ \end{array}\text{-O}\right]_n\text{-H}$ P3929-(PLLA5)	7.2	1.10	51.79	148.99	58.85	100.85	49.88	11.27
$\text{CH}_2\text{-O-CH}_2\text{-CH}_2\text{-O-CH}_2\text{-CH}_2\text{-O-}\left[\text{C}\begin{array}{c} \text{O} \\ \parallel \\ \text{C} \end{array}\text{-CH}\begin{array}{c} \text{CH}_3 \\ \end{array}\text{-O}\right]_n\text{-H}$ P3938-(PLLA6)	17.5	1.15	62.54	173.98	60.54	105.71	44.82	16.90
$\text{CH}_2\text{-O-CH}_2\text{-CH}_2\text{-O-CH}_2\text{-CH}_2\text{-O-}\left[\text{C}\begin{array}{c} \text{O} \\ \parallel \\ \text{C} \end{array}\text{-CH}\begin{array}{c} \text{CH}_3 \\ \end{array}\text{-O}\right]_n\text{-H}$ P6465-(PLLA7)	19	1.95	64.20	172.12	51.76	106.44	42.75	9.69
$\text{H-O-}\left[\text{C}\begin{array}{c} \text{O} \\ \parallel \\ \text{C} \end{array}\text{-CH}\begin{array}{c} \text{CH}_3 \\ \end{array}\text{-O}\right]_n\text{-H}$ P3934-(PLLA8)	27.5	1.12	66.83	179.09	70.59	109.34	42.35	30.37
$\text{CH}_2\text{-O-CH}_2\text{-CH}_2\text{-O-CH}_2\text{-CH}_2\text{-O-}\left[\text{C}\begin{array}{c} \text{O} \\ \parallel \\ \text{C} \end{array}\text{-CH}\begin{array}{c} \text{CH}_3 \\ \end{array}\text{-O}\right]_n\text{-H}$ P2290-(PLLA9)	40.4	1.35	62.71	180.57	50.06	101.63	10.01	43.06
$\text{CH}_2\text{-O-CH}\begin{array}{c} \text{CH}_3 \\ \end{array}\text{-O-}\left[\text{C}\begin{array}{c} \text{O} \\ \parallel \\ \text{C} \end{array}\text{-CH}\begin{array}{c} \text{CH}_3 \\ \end{array}\text{-O}\right]_n\text{-H}$ P6467-(PLLA10)	150	1.70	62.69	179.78	42.08	98.38	03.38	56.67

Table 1b Characteristics of PLA (*DL*-form) samples

Product ID	$M_n \cdot 10^3$	M_w/M_n	$T_g/^\circ\text{C}$
P8860-(PDLLA1)	0.95	1.15	-6.67
P8861-(PDLLA2)	3.0	1.12	26.24
P8862-(PDLLA3)	4.9	1.08	42.11
P8863-(PDLLA4)	8.5	1.05	46.12
P6464-(PDLLA5)	250	1.80	50.86

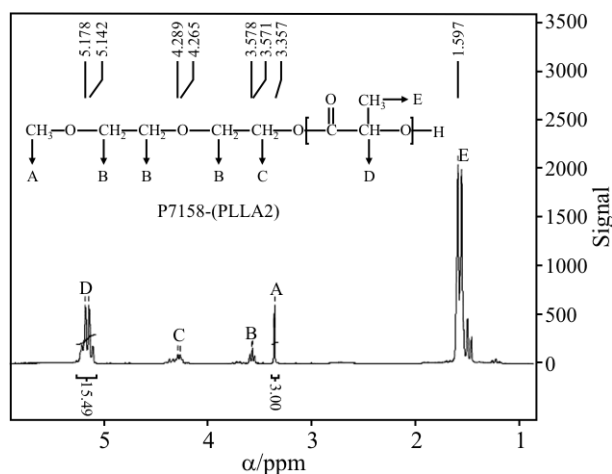
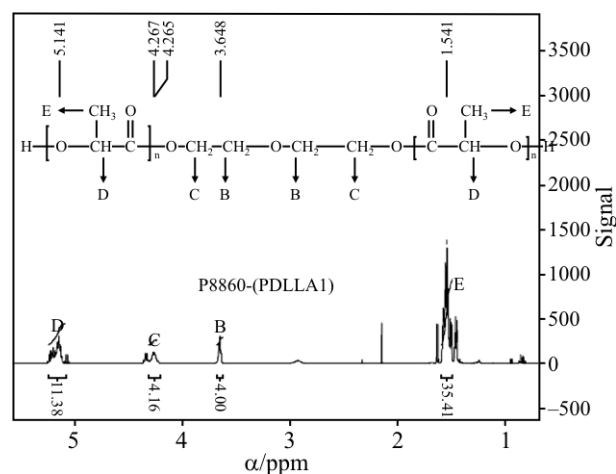
Characterization of materials

Both number average (M_n) and the mass average (M_w) molecular masses were determined by size exclusion chromatography (SEC) on a Varian instrument equipped with refractive index, UV and dual detectors from Viscotek Co. (light scattering, and viscosity detectors). All three columns were procured from Supelco (G6000-4000, 2000-HXL) and used for the SEC at 35°C where THF was used as the eluent containing 4.0 triethyl amine ($V/V\%$). The light scattering detectors were calibrated with polylactide standards. The molecular masses of the obtained polymers were further verified by their ^1H NMR spectra by comparing the integration values from the initiator moiety and from lactide units. The values were found close in agreement with the SEC results. Two representatives ^1H NMR spectra for lactide samples (PLLA2 and

PDLLA1) are presented in Fig. 1. The number-average molecular mass and polydispersity index (M_w/M_n) of PLA samples (*L* and *DL*) used in this study are given in Tables 1a and b, respectively.

Measurement of properties

Thermal analysis was carried out with a TA Q100 Differential Scanning Calorimeter (DSC) (TA Instruments) which was calibrated against an indium standard. An empty aluminum pan was the reference. The samples (6–8 mg) were run at a 10°C min⁻¹ heating/cooling ramp in two heating-cooling cycles in a nitrogen atmosphere (flow rate 50 mL min⁻¹). In the first cycle, PLA samples were heated from -20 to 200°C and isothermed for 5 min; cooled back to -20°C and isothermed for 2 min. Same steps were fol-


Fig. 1a ^1H NMR spectra of poly(lactide) samples PLLA2

Fig. 1b ^1H NMR spectra of poly(lactide) samples PDLLA1

lowed in the second cycle. The melting temperature (T_m) was taken at the end of the melting peak. The crystallization temperature (T_c) was considered as the minimum of the exothermic peak. The T_m was determined from the first heating cycle while crystallization and glass transition temperature were calculated by the second heating-cooling cycle. The area under the curve was calculated as the enthalpy from the instrument software. The non-isothermal crystallization studies were carried out in the cooling rate ranged from 2.5 to 20°C min⁻¹. For PLA samples containing racemic mixture (*DL*) were annealed at 200°C for 5 min and cooling–heating cycle was followed to locate the glass transition temperature. Thermal scans for each sample were carried out in duplicate and the average values are reported in this paper.

Fourier transform infrared spectra were obtained with a FTIR spectrophotometer (Nicolet-Avatar 330 model) using He–Ne laser by the transmission method. Polylactide samples were cast onto KBr crystal from solutions in chloroform, and the solvent was evaporated prior to measurement. No evidence of residual solvent was observed spectroscopically. Spectra were recorded in the range 400–4000 cm⁻¹. The instrument settings were kept constant (16 scans; resolution, 4 cm⁻¹; velocity, 0.6329; aperture, 100).

Results and discussion

Thermal behaviors of polylactides *L* and *DL* isomers are presented in Table 1. The glass transition temperature of semi-crystalline *L*-isomer increased from -3.8 to 66.8°C as number-average molecular mass was increased from 550 to 27500 and leveled thereafter (Table 1a). A lowering of glass transition temperature was pronounced for high molecular mass samples (PLLA9 and 10) which is probably affected by the high polydispersity index and the plasticizing effect contributed by low molecular mass polymers. The T_g of *DL* form increased systematically from -6.7 to about 50.9°C with an increase of M_n from about 1000 to 250000. The glass transition temperature of *L* form showed slightly higher values than *DL* form. This trend is very common for polymeric materials that bear crystallinity.

It is observed that each PLLA sample exhibits an endothermic melting peak during the thermal scan except the low molecular mass sample (PLLA1). The melting temperature (T_m) and enthalpy of crystal fusion (ΔH_m) of PLLA samples increased with M_n from 88 to 181°C and from 23.4 to 70.6 J g⁻¹, respectively. Samples with high polydispersity index exhibited lowering of ΔH_m though the melting temperature leveled (Table 1a). The melting temperature range and enthalpy obtained in this study are close in agreement with earlier observa-

tion for PLA [17]. PLLA samples exhibit crystallinity, however, no exothermic peak of crystallization was found for low molecular mass (550 to 1400) samples (Fig. 2). Low molecular mass polymers (short chains) are generally weaker in strength. Although they are crystalline, only weak Van der Waals forces hold the lattice together. This allows the crystalline layers to slip past one another causing a break in the material and causes the absence of distinct crystalline peak for low molecular mass PLA samples.

PLA samples with high M_n (>40000) significantly affected the crystallization behavior and showed lower crystallization temperature (T_c) and enthalpy associated with the crystallization (ΔH_c). The crystallization peaks attributed by both PLLA9 and PLLA10 were relatively lower (10°C min⁻¹). The crystallization peak was untraceable in the second scan even at excessive high cooling rate (40°C min⁻¹). The latter indicates that the molecular mobility of high molecular mass polymers became restricted dur-

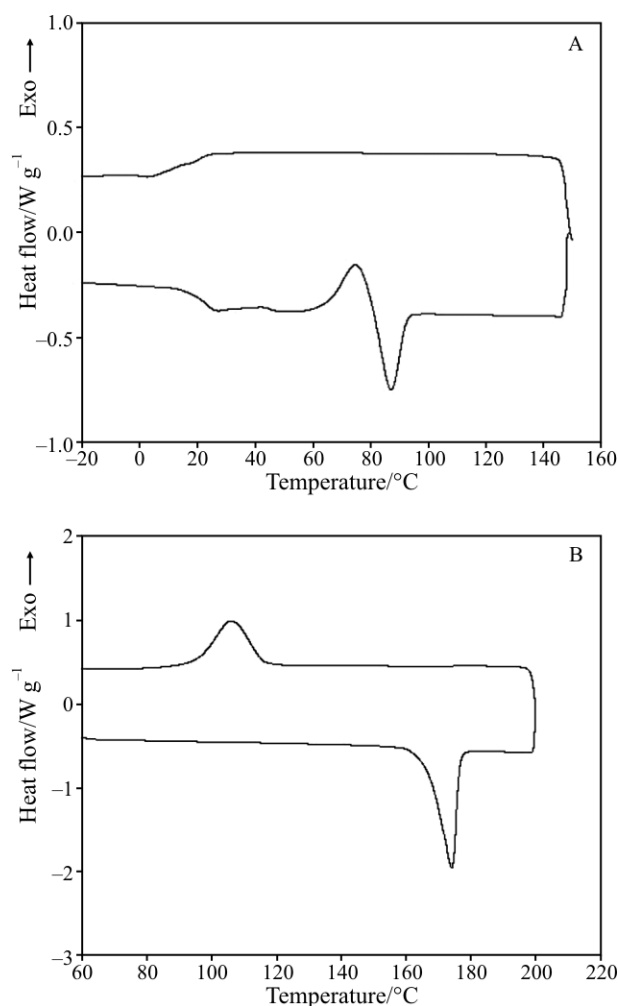


Fig. 2 Effect of number average molecular mass (M_n) on heating-cooling curves of PLLA2 and PLLA6; A – M_n of 1100 and B – M_n of 25000

ing high cooling rate and could not achieve the desired crystallinity during cooling of the melt.

The degree of crystallinity (χ_c) of PLA samples can be calculated based on the enthalpy value of a 100% crystalline PLA sample [18] from the following equation:

$$\% \chi_c = \frac{(\Delta H_m - \Delta H_c)}{93} \cdot 100$$

where ΔH_m is the melting enthalpy, ΔH_c is the crystallization enthalpy and 93 J g⁻¹ the melting enthalpy of totally crystallized PLA sample. This calculation leads to degree of crystallinity ranging from 8.3 to 56.7%. The degree of crystallinity values is close in agreement with the earlier reported values for PLA samples [17].

The thermal behavior of the polylactides depends on the thermal history of the samples and rate of heating. Figure 3 shows the typical heating-cooling pattern for PLLA sample at two selected heating rates (10 and 20°C min⁻¹). The melting peak is very sharp at a higher heating rate as compared to lower one. At a slower heating rate (10°C min⁻¹), the melting of PLLA was noticed at about 160°C with relatively low enthalpy of crystal fusion ($\Delta H_m = 58.5$ J g⁻¹) and the corresponding values at higher heating rate were 163°C and 59.4 J g⁻¹, respectively. While the sample was cooled from the melt at two different cooling rates, a higher crystallization exothermic peak at 108.3°C was observed for a cooling rate of 10 over 20°C min⁻¹ (102.4°C). The corresponding crystallization enthalpies equaled about 48.2 and 45.6 J g⁻¹, respectively.

Table 2 and Fig. 4 demonstrate that the non-isothermal melt-crystallization of polylactides is a function of cooling rate. As the cooling rate gradually increased from 2.5 to 20°C min⁻¹, the crystallization temperature (T_c) and associated enthalpy (ΔH_c) were

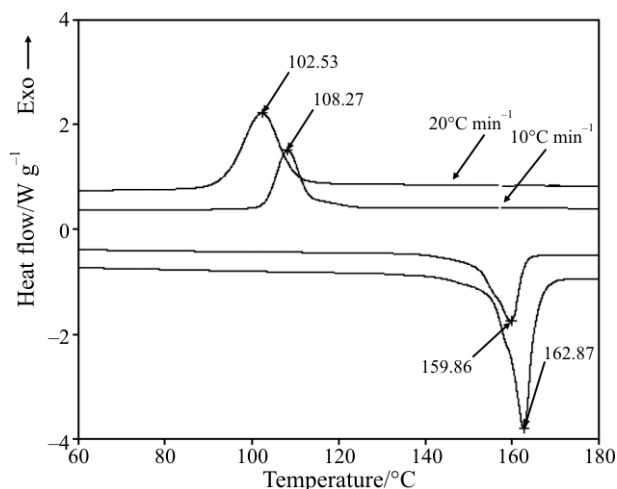


Fig. 3 Effect of heating rate on melting and crystallization of PLLA11

Table 2 Effect of heating rate on non-isothermal crystallization of PLA Sample ID # P3938 (PLLA7 and $M_n=17500$)

Heating rate/°C min ⁻¹	T_c /°C	ΔH_c /J g ⁻¹	χ_c /%
2.5	123.2	55.8	6.7
5	115.3	50.4	9.4
10	109.0	46.6	11.7
20	101.8	23.9	32.9

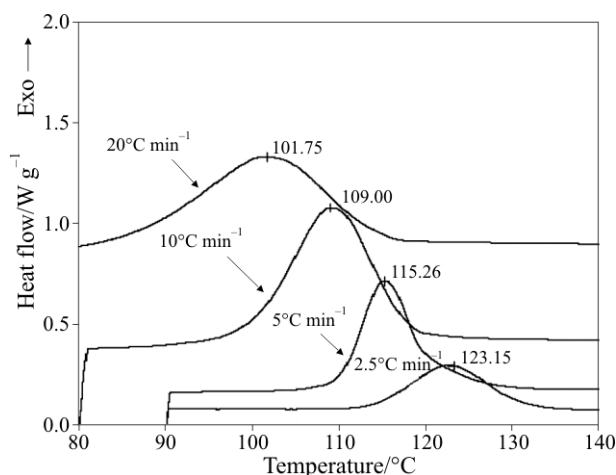


Fig. 4 Effect of cooling rate on crystallization of PLLA6

found to decrease significantly. It has been observed that the crystallization peak temperature increased and shifted towards a lower value as cooling rate was increased. This observation is very common for the crystallization of polymeric materials and the phenomenon can be attributed to the kinetic effect in a nucleation-controlled region [19]. At a lower cooling rate, there is sufficient time for the nuclei with a larger size that could stabilize at a higher temperature. On the other hand, at a fast cooling rate the polymer molecules experienced rapid decrease in temperature and produce fine nuclei that could stabilize at considerably lower temperature. A 2nd order polynomial equation can be used to predict the crystallization temperature-cooling rate behavior of PLA samples.

$$T_c = 0.07 \left(\frac{dT}{dt} \right)^2 - 2.75 \left(\frac{dT}{dt} \right) + 128.75 \quad (R^2=0.99)$$

The degree of crystallinity ($\% \chi_c$) was increased linearly from 6.7 to 33% as a function of cooling rate and the observation is supported by earlier reported values [17].

A comparison of thermal properties among *D* isomer, *L* isomer and racemic mixture (*DL*) of PLA is presented in Table 3. Both *D* and *L* isomers exhibited semi-crystalline behavior with possession of both melting and glass transition temperature. It is evident

Table 3 Effect of isomer on thermal properties of PLA

Product ID	M_n $\cdot 10^3$	M_w / M_n	Isomer	T_g / $^{\circ}\text{C}$	T_m / $^{\circ}\text{C}$	ΔH / J g^{-1}	T_c / $^{\circ}\text{C}$	ΔH / J g^{-1}
P3937-(PLLA4) $\text{CH}_3\text{-O-CH}_2\text{-CH}_2\text{-O-CH}_2\text{-CH}_2\text{-O-}\left[\text{C}\left(\begin{array}{c} \text{O} \\ \parallel \\ \text{C} \end{array}\right)\text{-CH}\left(\begin{array}{c} \text{CH}_3 \\ \end{array}\right)\text{-O}\right]_n\text{-H}$	4.7	1.09	<i>L</i>	45.60	157.82	55.50	98.25	47.82
P7052-(PDLLA6) $\text{CH}_3\text{-O-CH}_2\text{-CH}_2\text{-O-CH}_2\text{-CH}_2\text{-O-}\left[\text{C}\left(\begin{array}{c} \text{O} \\ \parallel \\ \text{C} \end{array}\right)\text{-CH}\left(\begin{array}{c} \text{CH}_3 \\ \end{array}\right)\text{-O}\right]_n\text{-H}$	4.3	1.90	<i>DL</i>	44.70	–	–	–	–
P3936-(PLLA11) $\text{CH}_3\text{-O-CH}_2\text{-CH}_2\text{-O-CH}_2\text{-CH}_2\text{-O-}\left[\text{C}\left(\begin{array}{c} \text{O} \\ \parallel \\ \text{C} \end{array}\right)\text{-CH}\left(\begin{array}{c} \text{CH}_3 \\ \end{array}\right)\text{-O}\right]_n\text{-H}$	7.0	1.09	<i>L</i>	67.94	159.87	58.78	108.28	48.31
P7379-(PDLLA7) $\text{H-}\left[\text{O-CH}\left(\begin{array}{c} \text{CH}_3 \\ \end{array}\right)\text{-C}\left(\begin{array}{c} \text{O} \\ \parallel \\ \text{C} \end{array}\right)\right]_n\text{-O-CH}_2\text{-CH}_2\text{-O-CH}_2\text{-CH}_2\text{-O-}\left[\text{C}\left(\begin{array}{c} \text{O} \\ \parallel \\ \text{C} \end{array}\right)\text{-CH}\left(\begin{array}{c} \text{CH}_3 \\ \end{array}\right)\text{-O}\right]_n\text{-H}$	7.3	1.16	<i>DL</i>	44.14	–	–	–	–
P3922-(PDLA1) $\text{CH}_3\text{-O-CH}_2\text{-CH}_2\text{-O-CH}_2\text{-CH}_2\text{-O-}\left[\text{C}\left(\begin{array}{c} \text{O} \\ \parallel \\ \text{C} \end{array}\right)\text{-CH}\left(\begin{array}{c} \text{CH}_3 \\ \end{array}\right)\text{-O}\right]_n\text{-H}$	13.8	1.19	<i>D</i>	65.69	170.26	67.01	107.57	52.38
P3936-(PLLA12) $\text{CH}_3\text{-O-CH}_2\text{-CH}_2\text{-O-CH}_2\text{-CH}_2\text{-O-}\left[\text{C}\left(\begin{array}{c} \text{O} \\ \parallel \\ \text{C} \end{array}\right)\text{-CH}\left(\begin{array}{c} \text{CH}_3 \\ \end{array}\right)\text{-O}\right]_n\text{-H}$	14.0	1.12	<i>L</i>	66.83	173.26	61.07	110.27	48.12
P3923-(PDLA2) $\text{CH}_3\text{-CH}\left(\begin{array}{c} \text{CH}_3 \\ \end{array}\right)\text{-O-}\left[\text{C}\left(\begin{array}{c} \text{O} \\ \parallel \\ \text{C} \end{array}\right)\text{-CH}\left(\begin{array}{c} \text{CH}_3 \\ \end{array}\right)\text{-O}\right]_n\text{-H}$	16.5	1.20	<i>D</i>	69.10	173.49	64.55	109	51.60
P2293-(PLLA13) $\text{CH}_3\text{-CH}\left(\begin{array}{c} \text{CH}_3 \\ \end{array}\right)\text{-O-}\left[\text{C}\left(\begin{array}{c} \text{O} \\ \parallel \\ \text{C} \end{array}\right)\text{-CH}\left(\begin{array}{c} \text{CH}_3 \\ \end{array}\right)\text{-O}\right]_n\text{-H}$	16.8	1.32	<i>L</i>	58.64	173.42	61.38	105	38.14

Table 4 Effect of end group on thermal properties of PLA

$\text{CH}_3\text{-O-CH}_2\text{-CH}_2\text{-O-CH}_2\text{-CH}_2\text{-O-}\left[\text{C}\left(\begin{array}{c} \text{O} \\ \parallel \\ \text{C} \end{array}\right)\text{-CH}\left(\begin{array}{c} \text{CH}_3 \\ \end{array}\right)\text{-O}\right]_n\text{-H}$	M_n $\cdot 10^3$	M_w / M_n	<i>R</i> group*	T_g / $^{\circ}\text{C}$	T_m / $^{\circ}\text{C}$	ΔH / J g^{-1}	T_c / $^{\circ}\text{C}$	ΔH / J g^{-1}
P7150- (PLLA3) $\text{CH}_3\text{-CH}\left(\begin{array}{c} \text{CH}_3 \\ \end{array}\right)\text{-O-}\left[\text{C}\left(\begin{array}{c} \text{O} \\ \parallel \\ \text{C} \end{array}\right)\text{-CH}\left(\begin{array}{c} \text{CH}_3 \\ \end{array}\right)\text{-O}\right]_n\text{-H}$	1.4	1.12	2	30.75	112.27	41.02	–	–
P8030-(PLLA14) $\text{CH}_3\text{-CH}\left(\begin{array}{c} \text{CH}_3 \\ \end{array}\right)\text{-O-}\left[\text{C}\left(\begin{array}{c} \text{O} \\ \parallel \\ \text{C} \end{array}\right)\text{-CH}\left(\begin{array}{c} \text{CH}_3 \\ \end{array}\right)\text{-O}\right]_n\text{-H}$	1.4	1.13	1	37.66	136.67	44.20	100.15	41.93
P2283- (PLLA15) $\text{CH}_3\text{-O-CH}_2\text{-CH}_2\text{-O-CH}_2\text{-CH}_2\text{-O-}\left[\text{C}\left(\begin{array}{c} \text{O} \\ \parallel \\ \text{C} \end{array}\right)\text{-CH}\left(\begin{array}{c} \text{CH}_3 \\ \end{array}\right)\text{-O}\right]_n\text{-H}$	24.6	1.33	1	68.31	178.48	56.61	136.68	55.80
P3938-(PLLA6) $\text{CH}_3\text{-O-CH}_2\text{-CH}_2\text{-O-CH}_2\text{-CH}_2\text{-O-}\left[\text{C}\left(\begin{array}{c} \text{O} \\ \parallel \\ \text{C} \end{array}\right)\text{-CH}\left(\begin{array}{c} \text{CH}_3 \\ \end{array}\right)\text{-O}\right]_n\text{-H}$	25.0	1.15	2	62.54	179.09	70.59	109.34	42.35

*1: $R=\text{CH}_3\text{-CH}(\text{CH}_3)\text{-O-}$ 2: $R=\text{CH}_3\text{-O-CH}_2\text{-CH}_2\text{-O-}$

from the table that there is no significant difference in thermal properties of PLA samples with almost equal molecular mass although their polydispersity indexes are different. It infers that thermal properties of PLA are dictated by lactyl unit not by the isomer. *DL* samples exhibited amorphous behavior with distinct glass transition temperature.

Effect of microstructure on the thermal behavior of *L*-polylactide is presented in Table 4. A relatively lower T_g and T_m values were observed for PLLA3 compared to PPLA14 although both had similar molecular masses. Additionally, PLLA3 failed to demonstrate the crystallinity and no distinct crystallization exotherm was found for the sample. The crystallization behavior of high molecular mass PLLA samples (PLLA15 and PLLA6) differed significantly where as both showed similar T_g and T_m . This finding confirmed that the microstructure played a significant role in crystallization process and crystallinity of polylactides.

Figure 5 shows the FTIR spectra (from 1300–1150 cm^{-1} in wavelength) of selected PLA samples. The spectrum of both *D* and *L* isomer of PLA (PLLA13 and PDLA2) are almost identical. Bands at 1269 and 1215–1186 cm^{-1} are known as crystalline bands in PLLA structures. These consist of vibrational components i.e., C–COO stretching, O–CH stretching, CH_3 rocking, and CH bending [20]. Both *D* and *L* samples exhibited a shoulder between 1240 and 1200 cm^{-1} that clearly distinguished from the *DL* sample (PDLLA8) where the shoulder was not present. A small shift of the crystalline band might be affected by preparation of sample, molecular mass and other factors. The absence of crystalline band in low molecular mass sample between 1215 and 1186 cm^{-1} justifies the absence of crystallinity. These observa-

tions are duly supported by earlier FTIR work on PLA samples [21].

Conclusions

Thermal analysis of a series of polylactides indicated that the microstructure, number average molecular mass and isomer type have considerable effects on glass transition temperature, melting and crystallization behavior. Semi-crystalline polylactides showed higher T_g over amorphous sample at similar M_n range and the T_g leveled at higher M_n . Lower molecular mass semi-crystalline samples did not exhibit melting and crystalline peak during thermal scan whereas, significant drop in crystallization temperature and crystallization enthalpy were observed for high molecular mass polylactides. Cooling rate significantly affected the degree of crystallinity from the melt and the crystalline peak was untraceable at higher cooling rate. A 2nd order polynomial equation has been proposed to predict the crystallization temperature-cooling rate behavior of PLA samples. DSC observation of crystallinity was supported by FTIR spectra between 1186 and 1269 cm^{-1} .

Acknowledgements

The authors wish to acknowledge Ms. Neelima Agarwal for locating the financial support from Polymer Source under the on-going research and development program for the synthesis of new materials. Terry Varshney is appreciated for editing the manuscript.

References

- 1 L. J. Fetters, D. J. Lohse, D. Richter, T.A. Witten and A. Zirkel, *Macromol.*, 27 (1994) 4639.
- 2 A. Tullo, *Chem. Eng. News*, 78 (2000) 13.
- 3 S. K. Varshney, O. Hnojewyj, J. Zhang and P. Rivelli, US Patent Application. 0225472, 2007.
- 4 R. G. Sinclair, *J. Macromol. Sci., Part A: Pure Appl. Chem.*, 33 (1996) 585.
- 5 J. Kline and H. H. Kline, *Die Makromol. Chem.*, 30 (1959) 23.
- 6 V. C. Schulz and J. J. Schwaab, *Die Makromol. Chem.*, 87 (1965) 90.
- 7 K. Jamshidi, S. H. Hyon and Y. Ikada, *Polymer*, 29 (1998) 2229.
- 8 M. Varma-Nair, R. Pan and B. J. Wunderlich, *J. Polymer Sci. Part B: Polym. Phys.*, 29 (1991) 1107.
- 9 H. Tsuji and Y. Ikada, *Polymer*, 36 (1995) 2709.
- 10 S. Brochu, R. E. Prud'homme, I. Barakat and R. Jérôme, *Macromol.*, 28 (1995) 5230.

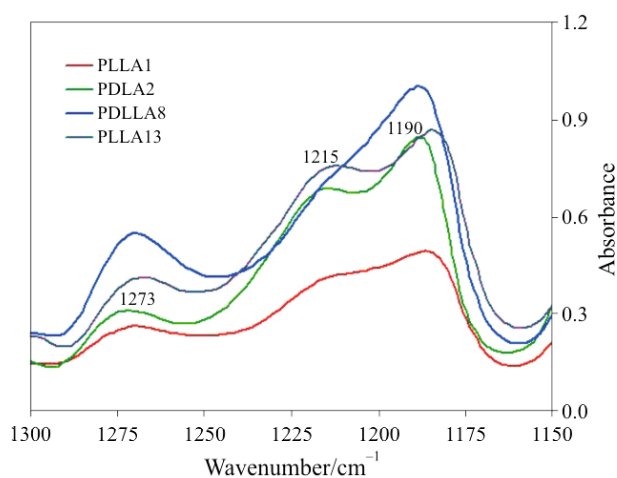


Fig. 5 FTIR spectra for selected PLA samples

- 11 K. A. M. Thakur, R. T. Kean, E. S. Hall, J. J. Kolstad, T. A. Lindgren, M. A. Doscotch, J. I. Siepmann and E. J. Munson. *Macromol.*, 29 (1996) 8844.
 - 12 H. Tsuji, F. Horii, M. Nakagawa, Y. Ikada, H. Odani and R. Kitamaru. *Macromol.*, 25 (1992) 4114.
 - 13 B. Kalb and A. J. Penings, *Polymer*, 21 (1980) 607.
 - 14 G. Perego, G. D. Cella and C. Bastioli, *J. Appl. Polym. Sci.*, 59 (1996) 37.
 - 15 M. Day, A. V. Nawaby and X. Liao, *J. Therm. Anal. Cal.*, 86 (2006) 623.
 - 16 M. Pyda, *The Nature of Biological Systems as Revealed by Thermal Methods*, D. Lőrinczy, Ed., Kluwer Academic Publisher, Amsterdam 2004.
 - 17 J. R. Sarasua, R. E. Prud'homme, M. Wisniewski, A. Le Borgne and N. Spassky, *Macromol.*, 31 (1998) 3895.
 - 18 E. W. Fischer and H. J. Sterzel Wegner, *Z. Kolloid. Polym.*, 251 (1973) 980.
 - 19 P. Supaphol, P. Thanomkiat, J. Junkasem and R. Dangtangee, *Polymer Test.*, 26 (2007) 20.
 - 20 S. H. Kang, S. L. Hsu, H. D Stidham, P. B. Smith, M. A. Leugers and X. Yang, *Macromol.*, 34 (2001) 4542.
 - 21 H. Urayama, S. I. Moon and Y. Kimura., *Macromol. Mater. Eng.*, 288 (2003) 137.
-
- Received: January 25, 2008
Accepted: July 10, 2008
OnlineFirst: November 12, 2008
-
- DOI: 10.1007/s10973-008-9035-x